

# High-resolution fMRI using Accelerated EPIK for Enhanced Characterisation of Functional Areas at 3T

Seong Dae Yun<sup>1</sup> and N. Jon Shah<sup>1,2</sup>

<sup>1</sup>Institute of Neuroscience and Medicine, Medical Imaging Physics (INM-4), Forschungszentrum Juelich, Juelich, Germany, <sup>2</sup>Faculty of Medicine, Department of Neurology, JARA, RWTH Aachen University, Aachen, Germany

**Target Audience:** This work demonstrates the enhanced characterisation of functional area using high-resolution functional imaging at 3T and should be of significant interest to the fMRI community.

**Purpose:** The relatively high imaging speed of EPI has led to its widespread use in dynamic MRI studies such as functional MRI. With the current technological development, a single-shot EPI sequence can offer a spatial resolution of 2–3 mm in an acquisition time of 2–3 s for the whole human brain. This is sufficient for most fMRI applications, but not enough for the applications investigating relatively small functional areas. In this work, for precise examination of such small functional area, a high-resolution imaging method was developed based on EPI with Keyhole (EPIK)<sup>1</sup>. In the previous studies<sup>1–3</sup>, EPIK was shown to provide a higher temporal resolution and less image distortions than single-shot EPI whilst maintaining at least comparable performance for the detection of blood-oxygenated-level-dependent (BOLD)-based signals. Here, the EPIK scheme was further accelerated with parallel imaging and partial Fourier techniques to achieve even higher resolution. The performance of EPIK was directly compared to that of EPI (community standard) and its potential advantages were investigated with visual fMRI experiments.

**Methods:** A visual checkerboard paradigm was employed for *in vivo* fMRI experiments to elicit circumscribed activation in the visual cortex. The imaging protocol consisted of 6 dummy scans for reaching a steady state and 72 scans comprising six cycles of baseline-activation states, each lasting 6 volume acquisitions for a total of 18 seconds. Sixteen healthy volunteers (10 males, 6 females; mean age, 28.88 years; range, 20–42 years) participated in the study and written, informed consent was obtained. For each fMRI session, functional data were acquired using two sequences (EPI and EPIK) to evaluate the performance of EPIK in a direct comparison with EPI. After being accelerated with parallel imaging ( $R = 2$ ) and the partial Fourier ( $R = 8/6$ ) techniques, each sequence (EPI and EPIK) were optimised to offer its highest possible spatial resolution under the condition that the other imaging parameters were kept identical: FOV =  $240 \times 240 \text{ mm}^2$ , flip angle =  $90^\circ$ , TR/TE = 3000/35 ms and slice thickness = 4 mm with a distance factor of 10%. As a consequence, matrix size of  $240 \times 240$  ( $1.00 \times 1.00 \text{ mm}^2$ ) with 32 slices and matrix size of  $192 \times 192$  ( $1.25 \times 1.25 \text{ mm}^2$ ) with 28 slices were achieved by EPIK and EPI, respectively. The resolution enhancement achieved by EPIK was mostly attributed to its acquisition strategy. Figure 1 shows the schematic representation of the k-space trajectory for a three-shot EPIK sequence. Each measurement scans the central k-space region (k-space keyhole:  $K_K$ ) completely with  $\Delta k_y = 1/\text{FOV}$ , whilst the peripheral k-space regions (k-space sparse:  $K_S$ ) are sparsely sampled with  $\Delta k_y' = 3/\text{FOV}$  (SPARSE factor of 3). By sharing the sparse region data from three consecutive scans, with the keyhole region updated for every measurement, one obtains an image per TR excluding 2 initial dummy runs. Furthermore, this example features one-fourth of k-space as the keyhole region. Thus, the total number of phase encoding lines to be sampled reduces to  $1/2$  of that for comparable EPI. When a fourth scan is acquired, the peripheral k-space data from the first scan are discarded and thus the periphery,  $K_S$ , is updated by application of this sliding window. For this work, the above configuration was employed on a Magnetom Tim® Trio 3T MRI scanner (Siemens, Erlangen, Germany) with a 32-channel phased array coil from the manufacturer.

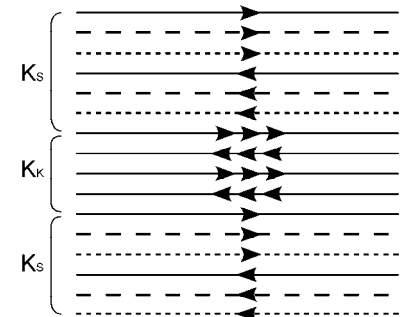


**Figure 1** Schematic representation for a three-shot EPIK sequence. The solid, dashed and fine-dashed lines in  $K_S$  regions indicate the sampling positions performed at the 1st, 2nd and 3rd measurements, respectively.

**Results:** Figure 2a and b show reconstructed *in vivo* slices with EPI and EPIK sequences. Visual inspection of the two slices suggests that both EPI and EPIK images were well reconstructed without any significant degradation of image quality. However, the EPIK image obviously exhibits enhanced spatial representation of the anatomical structures such as gyri or sulci when compared to the EPI image. In order to assess the differences in the activation patterns elicited by the two imaging sequences, first level baseline contrasts were calculated for each subject and were then taken to the second level. Two one-sample t-tests (one per sequence) were performed; for preprocessing and analysing fMRI data, SPM8 (Wellcome Department of Imaging Neuroscience, UCL, London, UK) was used here. Figure 3a and b show activation regions obtained with an uncorrected p-value  $< 0.001$  (t-value  $> 3.73$ ). For each method, the slice with the maximum t-value is presented and the range of t-values is given. In the next columns, the activation regions for the whole slices are presented in sagittal, coronal and axial views. Visual inspection of Figure 3 revealed that the activations were largely identified around the visual cortex in both imaging methods. Besides the visual cortex, although illustrating rather smaller area, the lateral geniculate nucleus (LGN) and superior colliculus (SC) were also recognized as activation regions. For more quantitative analysis on the obtained one-sample t-test results, statistical quantities such as maximum t-value, mean t-value and number of detected voxels were examined for several functional ROIs as listed in Table 1. The results for the visual cortex region (V1–V5) showed that EPIK recognized more activation regions than EPI, in terms of number of voxels activated, while maintaining the comparable maximum and mean t-values. Particularly for LGN (L), LGN (R) and SC (L) regions, EPIK achieved substantial improvements in yielding the maximum t-values as well as the number of detected voxels. Overall, LGN and SC regions were better characterised by EPIK than EPI.

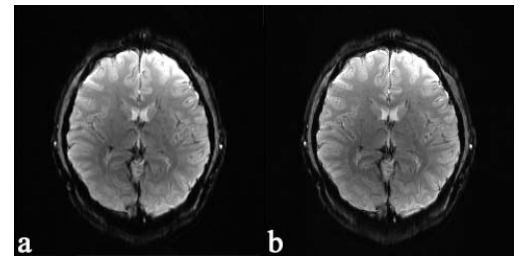


**Figure 2** High-resolution (a) EPI and (b) EPIK images

**Conclusions:** For enhanced detection of neural signals in fMRI, high-resolution EPIK has been demonstrated here at 3T. EPIK yielded higher resolution images with an increased brain coverage ( $1.00 \times 1.00 \text{ mm}^2$  with 32 slices) than EPI ( $1.25 \times 1.25 \text{ mm}^2$  with 28 slices) for comparable parameters. The advantages of EPIK over EPI stemming from the higher resolution were found particularly in the relatively small brain regions such as LGN and SC. **References:** 1. Zaitsev M, Zilles K, Shah NJ. Magn Reson Med 2001;45:109–117. 2. Zaitsev M, Arcey JD, Collins DJ, et al. Phys Med Biol 2005;50:4491–4505. 3. Yun S, Reske M, Vahedipour K, et al. NeuroImage 2013;73:135–143.

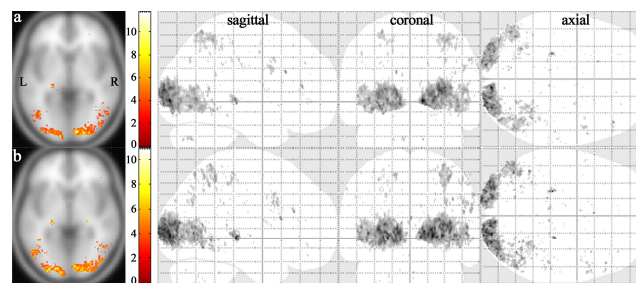


**Figure 3** One-sample t-test results (random effects; an uncorrected p-value  $< 0.001$ ) obtained from (a) EPI and (b) EPIK;

**Table 1** Statistical quantities (maximum & mean t-values and number of detected voxels) for several functional ROIs

ROI	Max t-val. (EPI/EPIK)	Mean t-val. (EPI/EPIK)	# of voxel (EPI/EPIK)
V1 (L,R)	11.73/10.36	5.25/5.35	2338/3472
V2 (L,R)	8.57/ 9.38	4.53/4.89	279/ 667
V3 (L,R)	9.73/ 8.98	5.00/4.93	2840/3705
V4 (L,R)	8.55/ 8.17	4.65/4.70	589/ 842
V5 (L,R)	6.22/ 8.09	4.25/4.39	459/ 607
LGN (L)	8.16/10.85	4.84/5.11	133/ 199
LGN (R)	4.08/10.21	4.08/5.51	1/ 60
SC (L)	4.52/ 5.17	4.15/4.28	9/ 41
SC (R)	6.49/ 4.93	4.68/4.26	13/ 22